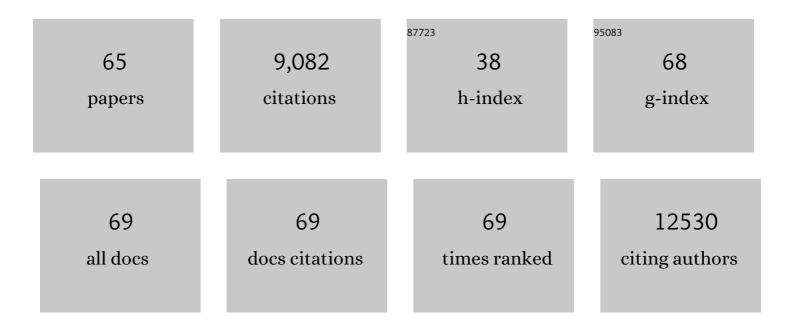
Li-Chang Yin

List of Publications by Year in descending order

Source: https://exaly.com/author-pdf/973086/publications.pdf Version: 2024-02-01



LI-CHANC YIN

#	Article	IF	CITATIONS
1	Efficient electrochemical reduction of CO to C2 products on the transition metal and boron co-doped black phosphorene. Chinese Chemical Letters, 2022, 33, 2183-2187.	4.8	26
2	Achieving efficient N2 electrochemical reduction by stabilizing the N2H* intermediate with the frustrated Lewis pairs. Journal of Energy Chemistry, 2022, 66, 628-634.	7.1	13
3	Monolayer MoSi2N4- as promising electrocatalyst for hydrogen evolution reaction: A DFT prediction. Journal of Materials Science and Technology, 2022, 99, 215-222.	5.6	31
4	A non-flammable hydrous organic electrolyte for sustainable zinc batteries. Nature Sustainability, 2022, 5, 205-213.	11.5	277
5	Constructing Anatase–Brookite TiO ₂ Phase Junction by Thermal Topotactic Transition to Promote Charge Separation for Superior Photocatalytic H ₂ Generation. Journal of Physical Chemistry Letters, 2022, 13, 4244-4250.	2.1	9
6	Surface Oxygen Vacancies Confined by Ferroelectric Polarization for Tunable CO Oxidation Kinetics. Advanced Materials, 2022, 34, e2202072.	11.1	13
7	Steering surface reconstruction of copper with electrolyte additives for CO2 electroreduction. Nature Communications, 2022, 13, .	5.8	47
8	Mechanistic insights into interfaces and nitrogen vacancies in cobalt hydroxide/tungsten nitride catalysts to enhance alkaline hydrogen evolution. Journal of Materials Chemistry A, 2021, 9, 11323-11330.	5.2	12
9	Catalytically Active Site Identification of Molybdenum Disulfide as Gas Cathode in a Nonaqueous Li–CO ₂ Battery. ACS Applied Materials & Interfaces, 2021, 13, 6156-6167.	4.0	18
10	Synergistic alloying effects on nanoscale precipitation and mechanical properties of ultrahigh-strength steels strengthened by Ni3Ti, Mo-enriched, and Cr-rich co-precipitates. Acta Materialia, 2021, 209, 116788.	3.8	54
11	Stability and Catalytic Performance of Single-Atom Catalysts Supported on Doped and Defective Graphene for CO ₂ Hydrogenation to Formic Acid: A First-Principles Study. ACS Applied Nano Materials, 2021, 4, 6893-6902.	2.4	40
12	Highly Polymerized Wine-Red Carbon Nitride to Enhance Photoelectrochemical Water Splitting Performance of Hematite. Journal of Physical Chemistry C, 2021, 125, 13273-13282.	1.5	15
13	Na–CO2 battery with NASICON-structured solid-state electrolyte. Nano Energy, 2021, 85, 105972.	8.2	29
14	An ultrasensitive molybdenum-based double-heterojunction phototransistor. Nature Communications, 2021, 12, 4094.	5.8	37
15	Search for an exotic parity-odd spin- and velocity-dependent interaction using a magnetic force microscope. Physical Review D, 2021, 104, .	1.6	9
16	Phosphorous-doped molybdenum disulfide anchored on silicon as an efficient catalyst for photoelectrochemical hydrogen generation. Applied Catalysis B: Environmental, 2020, 263, 118259.	10.8	40
17	A Universal Seeding Strategy to Synthesize Single Atom Catalysts on 2D Materials for Electrocatalytic Applications. Advanced Functional Materials, 2020, 30, 1906157.	7.8	91
18	Pushing the conductance and transparency limit of monolayer graphene electrodes for flexible organic light-emitting diodes. Proceedings of the National Academy of Sciences of the United States of America, 2020, 117, 25991-25998.	3.3	28

LI-CHANG YIN

#	Article	IF	CITATIONS
19	High-performance Na–CO ₂ batteries with ZnCo ₂ O ₄ @CNT as the cathode catalyst. Journal of Materials Chemistry A, 2020, 8, 23974-23982.	5.2	25
20	CdPS ₃ nanosheets-based membrane with high proton conductivity enabled by Cd vacancies. Science, 2020, 370, 596-600.	6.0	120
21	Composition dependent mobility and bandgaps in (La0.05Ba <i>x</i> Sr0.95â^' <i>x</i>)SnO3 epitaxial films. Applied Physics Letters, 2020, 117, .	1.5	2
22	Strain effect on the catalytic activities of B- and B/N-doped black phosphorene for electrochemical conversion of CO to valuable chemicals. Journal of Materials Chemistry A, 2020, 8, 11986-11995.	5.2	31
23	An Anionâ€Tuned Solid Electrolyte Interphase with Fast Ion Transfer Kinetics for Stable Lithium Anodes. Advanced Energy Materials, 2020, 10, 1903843.	10.2	186
24	Controlled Oneâ€pot Synthesis of Nickel Single Atoms Embedded in Carbon Nanotube and Graphene Supports with High Loading. ChemNanoMat, 2020, 6, 1063-1074.	1.5	14
25	Lithium Anodes: An Anionâ€Tuned Solid Electrolyte Interphase with Fast Ion Transfer Kinetics for Stable Lithium Anodes (Adv. Energy Mater. 14/2020). Advanced Energy Materials, 2020, 10, 2070063.	10.2	3
26	Nitrogen electroreduction performance of transition metal dimers embedded into N-doped graphene: a theoretical prediction. Journal of Materials Chemistry A, 2020, 8, 4533-4543.	5.2	124
27	The Regulating Role of Carbon Nanotubes and Graphene in Lithiumâ€ion and Lithium–Sulfur Batteries. Advanced Materials, 2019, 31, e1800863.	11.1	339
28	Single-Atom Mn–N ₄ Site-Catalyzed Peroxone Reaction for the Efficient Production of Hydroxyl Radicals in an Acidic Solution. Journal of the American Chemical Society, 2019, 141, 12005-12010.	6.6	203
29	An alkali metal–selenium battery with a wide temperature range and low self-discharge. Journal of Materials Chemistry A, 2019, 7, 21774-21782.	5.2	38
30	Photocharge Trapping in Two-Sheet Reduced Graphene Oxide–Ti _{0.87} O ₂ Heterostructures and Their Photoreduction and Photomemory Applications. ACS Applied Nano Materials, 2019, 2, 6378-6386.	2.4	6
31	Suppressing lithium dendrite formation by slowing its desolvation kinetics. Chemical Communications, 2019, 55, 13211-13214.	2.2	43
32	Interlayer epitaxy of wafer-scale high-quality uniform AB-stacked bilayer graphene films on liquid Pt3Si/solid Pt. Nature Communications, 2019, 10, 2809.	5.8	43
33	Alcohol-Guided Growth of Two-Dimensional Narrow-Band Red-Emitting K ₂ TiF ₆ :Mn ⁴⁺ for White-Light-Emitting Diodes. ACS Applied Materials & Interfaces, 2019, 11, 20143-20149.	4.0	33
34	B-terminated (111) polar surfaces of BP and BAs: promising metal-free electrocatalysts with large reaction regions for nitrogen fixation. Journal of Materials Chemistry A, 2019, 7, 13284-13292.	5.2	87
35	Homogeneous Doping of Substitutional Nitrogen/Carbon in TiO ₂ Plates for Visible Light Photocatalytic Water Oxidation. Advanced Functional Materials, 2019, 29, 1901943.	7.8	61
36	Lithium Batteries: The Regulating Role of Carbon Nanotubes and Graphene in Lithium–Ion and Lithium–Sulfur Batteries (Adv. Mater. 9/2019). Advanced Materials, 2019, 31, 1970066.	11.1	8

LI-CHANG YIN

#	Article	IF	CITATIONS
37	Frustrated Lewis pairs photocatalyst for visible light-driven reduction of CO to multi-carbon chemicals. Nanoscale, 2019, 11, 20777-20784.	2.8	38
38	An Aluminum–Sulfur Battery with a Fast Kinetic Response. Angewandte Chemie, 2018, 130, 1916-1920.	1.6	43
39	An Aluminum–Sulfur Battery with a Fast Kinetic Response. Angewandte Chemie - International Edition, 2018, 57, 1898-1902.	7.2	154
40	An Unusual Strong Visibleâ€Light Absorption Band in Red Anatase TiO ₂ Photocatalyst Induced by Atomic Hydrogenâ€Occupied Oxygen Vacancies. Advanced Materials, 2018, 30, 1704479.	11.1	231
41	Surface Chemistry in Cobalt Phosphide-Stabilized Lithium–Sulfur Batteries. Journal of the American Chemical Society, 2018, 140, 1455-1459.	6.6	393
42	Maximizing the visible light photoelectrochemical activity of B/N-doped anatase TiO2 microspheres with exposed dominant {001} facets. Science China Materials, 2018, 61, 831-838.	3.5	22
43	Amorphous Phosphorus-Doped Cobalt Sulfide Modified on Silicon Pyramids for Efficient Solar Water Reduction. ACS Applied Materials & Interfaces, 2018, 10, 37142-37149.	4.0	27
44	Unlocking Bifunctional Electrocatalytic Activity for CO ₂ Reduction Reaction by Win-Win Metal–Oxide Cooperation. ACS Energy Letters, 2018, 3, 2816-2822.	8.8	76
45	Rosin-enabled ultraclean and damage-free transfer of graphene for large-area flexible organic light-emitting diodes. Nature Communications, 2017, 8, 14560.	5.8	184
46	Conductive porous vanadium nitride/graphene composite as chemical anchor of polysulfides for lithium-sulfur batteries. Nature Communications, 2017, 8, 14627.	5.8	912
47	Ultrafast Growth of Highâ€Quality Monolayer WSe ₂ on Au. Advanced Materials, 2017, 29, 1700990.	11.1	139
48	Single-wall carbon nanotube network enabled ultrahigh sulfur-content electrodes for high-performance lithium-sulfur batteries. Nano Energy, 2017, 42, 205-214.	8.2	183
49	Molybdenum-doped ZnS sheets with dominant {1 1 1} facets for enhanced visible light photocatalytic activities. Journal of Colloid and Interface Science, 2017, 507, 200-208.	5.0	10
50	Kinetically Enhanced Electrochemical Redox of Polysulfides on Polymeric Carbon Nitrides for Improved Lithium–Sulfur Batteries. ACS Applied Materials & Interfaces, 2016, 8, 25193-25201.	4.0	149
51	Selective Breaking of Hydrogen Bonds of Layered Carbon Nitride for Visible Light Photocatalysis. Advanced Materials, 2016, 28, 6471-6477.	11.1	507
52	An Amorphous Carbon Nitride Photocatalyst with Greatly Extended Visibleâ€Lightâ€Responsive Range for Photocatalytic Hydrogen Generation. Advanced Materials, 2015, 27, 4572-4577.	11.1	771
53	Switching Photocatalytic H ₂ and O ₂ Generation Preferences of Rutile TiO ₂ Microspheres with Dominant Reactive Facets by Boron Doping. Journal of Physical Chemistry C, 2015, 119, 84-89.	1.5	18
54	Greatly Enhanced Electronic Conduction and Lithium Storage of Faceted TiO ₂ Crystals Supported on Metallic Substrates by Tuning Crystallographic Orientation of TiO ₂ . Advanced Materials, 2015, 27, 3507-3512.	11.1	79

LI-CHANG YIN

#	Article	IF	CITATIONS
55	Metal/Oxide Interface Nanostructures Generated by Surface Segregation for Electrocatalysis. Nano Letters, 2015, 15, 7704-7710.	4.5	233
56	Large-area synthesis of high-quality and uniform monolayer WS2 on reusable Au foils. Nature Communications, 2015, 6, 8569.	5.8	336
57	Visualizing the roles of graphene for excellent lithium storage. Journal of Materials Chemistry A, 2014, 2, 17808-17814.	5.2	48
58	Batteries: A Graphene–Pureâ€Sulfur Sandwich Structure for Ultrafast, Longâ€Life Lithium–Sulfur Batteries (Adv. Mater. 4/2014). Advanced Materials, 2014, 26, 664-664.	11.1	21
59	Carbon–sulfur composites for Li–S batteries: status and prospects. Journal of Materials Chemistry A, 2013, 1, 9382.	5.2	757
60	A red anatase TiO2 photocatalyst for solar energy conversion. Energy and Environmental Science, 2012, 5, 9603.	15.6	379
61	Crystal facet-dependent photocatalytic oxidation and reduction reactivity of monoclinic WO3 for solar energy conversion. Journal of Materials Chemistry, 2012, 22, 6746.	6.7	356
62	A flexible nanostructured sulphur–carbon nanotube cathode with high rate performance for Li-S batteries. Energy and Environmental Science, 2012, 5, 8901.	15.6	468
63	Heteroatomâ€Modulated Switching of Photocatalytic Hydrogen and Oxygen Evolution Preferences of Anatase TiO ₂ Microspheres. Advanced Functional Materials, 2012, 22, 3233-3238.	7.8	128
64	Polar interface-induced improvement in high photocatalytic hydrogen evolution over ZnO–CdS heterostructures. Energy and Environmental Science, 2011, 4, 3976.	15.6	147
65	Functional anion concept: effect of fluorine anion on hydrogen storage of sodium alanate. Physical Chemistry Chemical Physics, 2007, 9, 1499-1502	1.3	83